AD-A249 867

REGIONAL WAVE ATTENUATION IN EURASIA

Kin-Yip Chun
Tianfei Zhu

University of Toronto
Department of Physics
60 St George Street
Toronto, Ontario
M5S 1A7 Canada

DISTRIBUTION STATEMENT A
Approved for public release;
Distribution Unlimited

April 1992

Scientific Report Number 1
27 September 1991 - 31 March 1992

Approved for Public Release; Distribution Unlimited

Sponsored by
Defense Advanced Research Project Agency
Nuclear Monitoring Research Office
Contract Number: F29601-91-C-DB24

92-12442

92 5 03 043

REPORT DOCUMENTATION PAGE

Form Approved
OMB No. 0704-0188

Public reporting burden for this collection of information is estimated to average 1 hour per response, including the time for reviewing instructions, searching existing data sources, gathering and maintaining the data needed, and completing and reviewing the collection of information. Send comments regarding this burden estimate or any other aspect of this collection of information, including suggestions for reducing this burden, to Washington Headquarters Services, Directorate for Information Operations and Reports, 1215 Jefferson Davis Highway, Suite 1204, Arlington, VA 22202-4302, and to the Office of Management and Budget, Paperwork Reduction Project (0704-0188), Washington, DC 20503.

1. AGENCY USE ONLY (Leave blank)	2. REPORT DATE	3. REPORT TYPE AND DATES COVERED
	APRIL 1992	Semia Tech Rep 9/27/91-3/31/92

4. TITLE AND SUBTITLE
REGIONAL WAVE ATTENUATION IN EURASIA

5. FUNDING NUMBERS
F29601-91-C-DB24

6. AUTHOR(S)
KIN-YIP CHUN TIANFEI ZHU

7. PERFORMING ORGANIZATION NAME(S) AND ADDRESS(ES)
Geophysics Division, Department of Physics
University of Toronto
60 ST GEORGE STREET
TORONTO, ONTARIO M5S 1A7 CANADA

8. PERFORMING ORGANIZATION REPORT NUMBER
NA

9. SPONSORING/MONITORING AGENCY NAME(S) AND ADDRESS(ES)
DARPA/NMRO, 3701 North Fairfax Drive, Arlington VA 22203-1714
Contracting Officer Representative:
Dr. Alan S. Ryall

10. SPONSORING/MONITORING AGENCY REPORT NUMBER
NA

11. SUPPLEMENTARY NOTES

12a. DISTRIBUTION/AVAILABILITY STATEMENT
APPROVED FOR PUBLIC RELEASE
DISTRIBUTION UNLIMITED

12b. DISTRIBUTION CODE

13. ABSTRACT (Maximum 200 words)

Presented here in this Scientific Report Number 1 are the preliminary results of the first phase of our two-year investigation into the regional wave attenuation in Eurasia. Our first six-month effort has focused upon the L_g waves, as recorded by the IRIS and CDSN stations. A time-domain method for measuring the L_g attenuation has been developed and successfully tested in Eurasia, yielding stable results which are directly compatible with Nuttli's method for seismic magnitude/yield estimation. While continuing to refine our L_g results through improvements in path coverage and methodological upgrading, our future efforts will be directed at gaining a better understanding of the P_n attenuation in the region.

14. SUBJECT TERMS				15. NUMBER OF PAGES
Lg ATTENUATION EURASIA IRIS CDSN SOURCE EFFECTS				15
TIME-DOMAIN ANALYSIS			SITE EFFECTS	16. PRICE CODE
17. SECURITY CLASSIFICATION OF REPORT	18. SECURITY CLASSIFICATION OF THIS PAGE	19. SECURITY CLASSIFICATION OF ABSTRACT		20. LIMITATION OF ABSTRACT
Unclassified	Unclassified	Unclassified		SAR

NSN 7540-01-280-5500 Standard Form 298 (Rev. 2-89)
Prescribed by ANSI Std. Z39-18

Table of Contents:

1. Introduction 1

2. A Time-Domain Method for Measuring Regional L_g Attenuation 1

3. Preliminary L_g Attenuation Results from Eurasia 3

4. Conclusions 4

5. References 6

Accession For
NTIS GRA&I
DTIC TAB
Unannounced
Justification
By
Distribution/
Availability Codes
Dist | Avail and/or Special
A-1

SUMMARY

The pioneering work on L_g magnitude, initiated by Nuttli in the early 1970s, has been seen blossoming in recent years into notable advancements in the use of L_g amplitudes for precise explosion yield estimation (Nuttli, 1986, 1988), propelling intense search for a reliable L_gQ measurement method. Numerous recent publications on this subject involve mostly spectral analysis of L_g wave trains of varying, somewhat arbitrarily chosen group-velocity windows or fixed-length time windows (*e.g.*, Hasegawa, 1985; Chun *et al.*, 1987; Baumgardt and Ziegler, 1988; Sereno *et al.*, 1988; Sereno, 1990). This program seeks to determine, among others, reliable L_gQ in time domain for Eurasia, rendering the result more directly compatible with Nuttli's method of explosion yield estimation.

We report here a new time-domain method for measuring L_g attenuation. Termed source pair/receiver pair (SPRP) method, the salient features of this approach are: a) effective decontamination of recording site effects, and instrument response error; and b) effective removal of source excitation function. We also report our preliminary L_g attenuation measurement results for Eurasia based upon the data from the IRIS and CDSN stations. Short IRIS and CDSN network recording histories, high event trigger threshold for the latter, and sparse network station coverage are factors which limit the spatial resolution of our regional L_g attenuation measurement. Nevertheless, the application of our new methodology has yielded surprisingly robust regional results. The stability of the results implies higher attainable spatial resolution (fine-scale regionalization) as the L_g path coverage improves. The path coverage improvement will come about as a result of our continuing acquisition of new IRIS and CDSN data during the remaining 18-months period of our two-year research project, as well as the use of additional Chinese seismic data.

1. INTRODUCTION

In the area of regional verification of nuclear test ban treaty compliance the DARPA research program has focussed sharply in recent years upon the use of L_g phase for both source discrimination and explosion yield estimation. We note that L_gQ estimates derived from the observed spectral amplitudes abound in the published seismological literature. These estimates are most useful for the spectral-ratio types of explosion/earthquake source discrimination (*e.g.*, L_g/P_n). It appears, however, that L_gQ estimate obtained in the time domain, taking into consideration of the Airy phase nature of the L_g wave (*e.g.*, Nuttli, 1973; Campillo *et al.*, 1984), provides a more pertinent attenuation correction term in the magnitude/yield calculations (Francis Wu, personal communication, 1992). This is because the Nuttli's magnitude/yield calculations are based upon time-domain L_g amplitude measurements made at around 1-sec period rather than spectral amplitudes derived over finite time windows (*e.g.*, 17-sec and 34-sec window lengths were used in Hasegawa, 1985; 3.6-3.0 km/sec group velocity window was used in Sereno, 1990).

Here we describe a method for measuring L_g attenuation. We demonstrate the reliability as well as the flexibility of the method by applying it to 73 L_g recordings produced by 10 large-magnitude earthquakes and registered at 9 IRIS and CDSN stations (Table 1 and Figure 1). The L_gQ results presented in this report are of preliminary nature. More refined results on regional wave attenuation, including both L_g and P_n Q, will be presented in future reports.

2. A TIME-DOMAIN METHOD FOR MEASURING L_g ATTENUATION

In what follows we describe the source pair/receiver pair (SPRP) method for measuring regional L_g wave attenuation.

We denote by $A_{i,j}$ the time-domain L_g amplitude due to the i^{th} source and recorded at the j^{th} station. We assume, following Nuttli (1973) and inserting instrument amplification I_j with its attendant error, site amplification S_j, and source radiation pattern R_i, that $A_{i,j}$ can be parameterized as

$$A_{i,j} = A_i R_i I_j S_j d_{i,j}{}^{-1/3} (sin\Delta_{i,j})^{-1/2} e^{-\gamma d_{i,j}} \qquad (1)$$

where A_i is the source excitation, $d_{i,j}$ the epicentral distance in kilometers between the i^{th} source and j^{th} station, Δ is the same epicentral distance but measured in degrees, and γ the coefficient of anelastic attenuation. This coefficient is related to the quality factor $Q(f)$ by the equation

$$\gamma(f) = \frac{\pi f}{UQ(f)}, \tag{2}$$

where U is the L_g group velocity.

Consider the diagram in Figure 2 where sources 1 and 2, are aligned with stations 1 and 2 along a great-circle path (shown as a solid, horizontal line). This configuration is reminiscent of the reversed two-station method (RTSM) deployed by Chun *et al.* (1987), and Zhu *et al.* (1991) in their regional phase attenuation studies in eastern Canada - except for the fact that the two stations now straddle the source pair rather than the other way around. It can be readily shown that

$$\left(\frac{A_{2,1}}{A_{1,1}}\frac{A_{1,2}}{A_{2,2}}\right)\left(\frac{d_{2,1}}{d_{1,1}}\frac{d_{1,2}}{d_{2,2}}\right)^{1/3}\left(\frac{sin\Delta_{2,1}}{sin\Delta_{1,1}}\frac{sin\Delta_{1,2}}{sin\Delta_{2,2}}\right)^{1/2} = e^{-\gamma(D_1+D_2)}, \tag{3}$$

where $D_1 = d_{2,1} - d_{1,1}$ and $D_2 = d_{1,2} - d_{2,2}$.

Note that in taking the L_g amplitude ratio $A_{2,1}/A_{1,1}$, the site amplification S_1 and instrument response error (if any) at station 1 both vanish through self-cancellations. Likewise, all source excitation and radiation pattern terms are cancelled when the product is taken of the amplitude ratios $A_{2,1}/A_{1,1}$ and $A_{1,2}/A_{2,2}$. As indicated schematically in Figure 2, a partial L_g blockage occurring near a station (KIV in Figure 1 for instance) does not significantly affect our L_g attenuation measurements.

Calling the lefthand side of equation (3) Y and taking the logarithm on both sides lead to

$$logY = -\gamma logeD, \tag{4}$$

where $D = D_1 + D_2$.

For simplicity, we now make the usual assumptions that the source radiation pattern and the site amplification are both azimuth independent for the L_g wave (*e.g.*, Sereno, 1990; Bennett *et al.*, 1990). Such assumptions are reasonable since the L_g, being the superpositions of many different higher-mode surface waves, is presumably more capable of "smoothing" out the azimuth-dependent effects at the source and receiver ends than do the body waves. Under these assumptions, the sources and receivers are no longer required to be co-linear (see dashed propagation paths in Figure 2). Instead of a variation of the RTSM method, we call this generalized version source pair/receiver pair (SPRP) method. Equation (4), which describes a straight line with zero intercept on the Y-axis, remains applicable.

3. PRELIMINARY L_g ATTENUATION RESULTS IN EURASIA

Figure 3 shows four seismograms illustrative of the quality and the characteristics of the L_g signatures we have been analyzing. Two are IRIS (GAR and OBN) recordings and rest CDSN (HIA and BJI) recordings. All are vertical-component, broadband data sampled at 20 points/sec. Only distant (Δ from 2543 to 4964 km) recordings are sampled here to show that the L_g waves do propagate to far-regional distances.

The actual L_g amplitudes $A_{i,j}$, which we use in equations (3) and (4), are time-domain measurements made on narrowband-filtered (0.375 - 0.625 Hz) records (Figure 3). The center frequency for the filter is 0.5 Hz. The choice of this particular center frequency is based upon our observation that the signal-to-noise ratio (SNR) at 0.5 Hz is good for the selected propagation paths, long and short, while the SNR at 1-Hz frequency and higher is only good for the relatively short paths. The $A_{i,j}$ represent the maximum zero-to-peak (trough) L_g amplitudes taken in the group velocity window 3.5 to 3.2 km per second (see arrow pairs in Figure 3).

Shown in Figure 4a is a plot of measured $logY$ values versus D. All 73 paths are used in this plot. The slope of the fitted least-squares line, as discussed previously, is $-loge\gamma$. Because of our concerns for the potential presence of systematic bias in the observed $logY$, we choose not to fix the Y-intercept at the origin, as implied by equation (4). In other words, we effectively allow the Y-intercept to be a free parameter of the least-squares fit.

The slope of the least-squares line shown in the figure gives a value of $(1.129\pm0.062)\times10^{-3}$ for γ, which translates to a Q value of 398, assuming an L_g group velocity of 3.5 km/sec. Note that our derived Y-intercept is close to zero, as it should.

The analysis which led to the results shown in Figure 4a is then repeated with eight fewer propagation paths, each having crossed a known, near-station partial L_g blockage. For the L_g paths crossing the northern and southern Ural Mountain (Figure 1), the effects of L_g blockage are not evident, as seen on our filtered seismograms. The deleted ones are: a) five paths which traverse the Caspian Sea to reach the KIV station (Figure. 1); and b) three L_g paths which traverse northern Tibet to reach the KMI station. The purpose here is to examine the effects of near-station, partial L_g blockages on the measured L_g attenuation.

Figure 4b shows the plot of $logY$ versus D with the eight potentially problematic paths removed from Figure 1. The slope of the least-squares line now gives a value of $(1.045\pm0.078)\times10^{-3}$ for γ, which translates to a Q value of 429. The result given in Figure 4b is our preferred L_g attenuation estimate at 0.5 Hz.

The wide epicentral distance span (from about 500 to 5,000 km), necessitated by the large inter-station distances and non-ideal epicentral locations of the earthquakes, renders it impossible to study the frequency dependence of the L_gQ ($Q(f) = Q_0 f^{\alpha}$), since the

high-frequency signal energies are attenuated along the paths more rapidly than their low-frequency counterparts. Upon reaching a far-regional station, only the low-frequency part of the L_g signal energy survives. To estimate Q_0 (Q at 1 Hz), it is then necessary to know α. Our literature search reveals that in tectonic regions Q_0 is small and α is large, but that the opposite is true in stable regions. For example, the L_g Q_0 in the Great Basin is 206 and the α 0.68 (Chavez and Priestley, 1987); the corresponding values are 1,100 and 0.19 in eastern Canada (Chun et al., 1987). The α estimate by Given et al. (1990) for eastern Kazakhstan is 0.4. According to Mitchell (private communication, 1992), the α value for Eurasia, just north of Tibet, could be as high as 0.6. Assuming an intermediate α value of 0.5 for the study region, our preferred result ($L_gQ(0.5Hz)$ seen in Figure 4b would then imply a Q_0 value of 607, which is intermediate between 206 for the Great Basin (Chavez and Priestley, 1987) and 1,100 for the Canadian Shield (Chun et al., 1987).

4. CONCLUSIONS

We have introduced a new method for measuring regional L_g attenuation. Termed SPRP, this method requires no great-circle alignment for the seismic source and receiver pairs, and is hence far more flexible than the reversed two-station method (RTSM) of Chun et al. (1987). This flexibility allows L_g attenuation measurements to be made using passive, sparse recordings from a seismic network with only a brief recording history.

Like the RTSM, the SPRP method enables effective cancellations of the source excitation function, station site effects and is capable of handling near-station partial L_g blockage to some extent. We have successfully applied the SPRP method to broadband IRIS and CDSN data. As shown in Figure 4a and 4b, the source- and receiver-corrected observations are well-behaved and straightforward to interpret. The data scatter is small by normal standards. The L_gQ at 0.5 Hz is 429, implying a Q_0 value of 607 if α is taken to be 0.5, a value which is at midpoint between Given's (1990) value of 0.4 and Mitchell's (personal communication, 1992) suggested value of 0.6.

Compared with the RTSM, two notable drawbacks of the SPRP method are: a) it does not permit the annihilation of the source radiation pattern effects; and b) it is capable of measuring only regional attenuation, not path attenuation. We wish to point out, however, that for L_g waves, which consist of superpositions of higher-mode surface waves, the radiation pattern effects are probably not very important. Also, as more data accumulate with time, the path coverage will improve, making possible fine-scale L_g attenuation mapping and consequently the derivation of effective path attenuation.

Acknowledgements

We are indebted to the staff at the Center for Seismic Studies for providing us with valuable technical assistance and for meeting our constant data requests. We thank the Lawrence Livermore National Laboratory for letting us use the new UNIX SAC code. This work has benefitted from the advice and comments generously given to us by Douglas Baumgardt, Joe Bennett, Zoltan Der, Robert Herrmann, Keith McLaughlin, Brian Mitchell, and Francis Wu.

5. REFERENCES

Baumgardt, D. R., and K. A. Ziegler (1988). Spectral evidence of source multiplicity in explosions: Application to regional discrimination of earthquakes and explosions, *Bull. Seism. Soc. Am.*, **78** 1773-1795.

Bennett, T. J., Scheimer, J. F., Campanella, A. K., and Murphy, J. R. (1990). Regional discrimination research and methodology implementation: Analyses of CDSN and Soviet IRIS data, *S-CUBED Report SSS-TR-90-11757*, Technical Report on Contract No. F19628-89-C-0043.

Campillo, M., M. Bouchon, and B. Massinon (1984). Theoretical study of the excitation, spectral characteristics, and geometrical attenuation of regional seismic phases, *Bull. Seism. Soc. Am.*, **74**, 79-90.

Chavez, D. E., and Priestley, K. F. (1987). Apparent Q of P_g and L_g in the Great Basin, paper presented at 9th Annual DARPA/AFGL Seismic Research Symposium, June 1987.

Chun, K.-Y., G. F. West, R. J. Kokoski, and C. Samson (1987). A novel technique for measuring L_g attenuation - results from Eastern Canada between 1 to 10 Hz, *Bull. Seism. Soc. Am.*, **77**, 398-419.

Given, H. K., Tarasov, N. T., Zhuravlev, V., Vernon, F. L., Berger, J., and Nersesov, I. L. (1990). High-frequency seismic observations in eastern Kazakhstan, USSR, with emphasis on chemical explosion experiments, *J. Geophys. Res.*, **95**, 295-307.

Hasegawa, H. S. (1985). Attenuation of L_g waves in the Canadian Shield, *Bull. Seism. Soc. Am.*, **75**, 1569-1582.

Nuttli, O. W. (1973). Seismic wave attenuation and magnitude relations for eastern North America, *J. Geophys. Res.*, **78**, 876-885.

Nuttli, O. W. (1986). L_g magnitudes of selected east Kazakhstan underground explosions, *Bull. Seism. Soc. Am.*, **76**, 1241-1251.

Nuttli, O. W. (1988). L_g magnitudes and yield estimates of Novaya Zemlya nuclear explosions, *Bull. Seism. Soc. Am.*, **78**, 873-884.

Sereno, T. J., Bratt, S. R., and Bache, T. C. (1988). Simultaneous inversion of regional wave spectra for attenuation and seismic moment in Scandinavia, *J. Geophys. Res.*, **93**, 2019-2035.

Sereno, T. J. (1990). Frequency-dependent attenuation in eastern Kazakhstan and implications for seismic detection thresholds in the Soviet Union, *Bull. Seism. Soc. Am.*, **80**, 2089-2105.

Zhu, T., Chun, K.-Y., and Gordon, F. W. (1991). Geometrical spreading and Q of P_n waves: An investigative study in eastern Canada, *Bull. Seism. Soc. Am.*, **81**, 882-896.

TABLE 1

Event No.	Date	Origin Time (Hr:Min:Sec)	Latitude (N)	Longitude (E)	Depth (km)	Magnitude (mb)
1	14 Jun 1990	12:47:29	47.87	85.07	58	6.1
2	12 Nov 1990	12:28:52	42.96	78.07	19	5.9
3	25 Feb 1991	14:30:28	40.39	78.96	21	5.5
4	15 May 1990	22:29:59	36.11	100.12	14	5.5
5	26 Apr 1990	09:37:45	36.24	100.25	10	6.3
6	14 Jan 1990	03:03:19	37.82	91.97	12	6.1
7	22 Sep 1989	02:25:51	31.58	102.43	15	6.1
8	17 May 1989	05:04:36	57.09	122.02	31	5.6
9	20 Apr 1989	22:59:54	57.17	121.98	26	6.1
10	05 Mar 1990	20:47:01	36.91	73.02	12	5.8

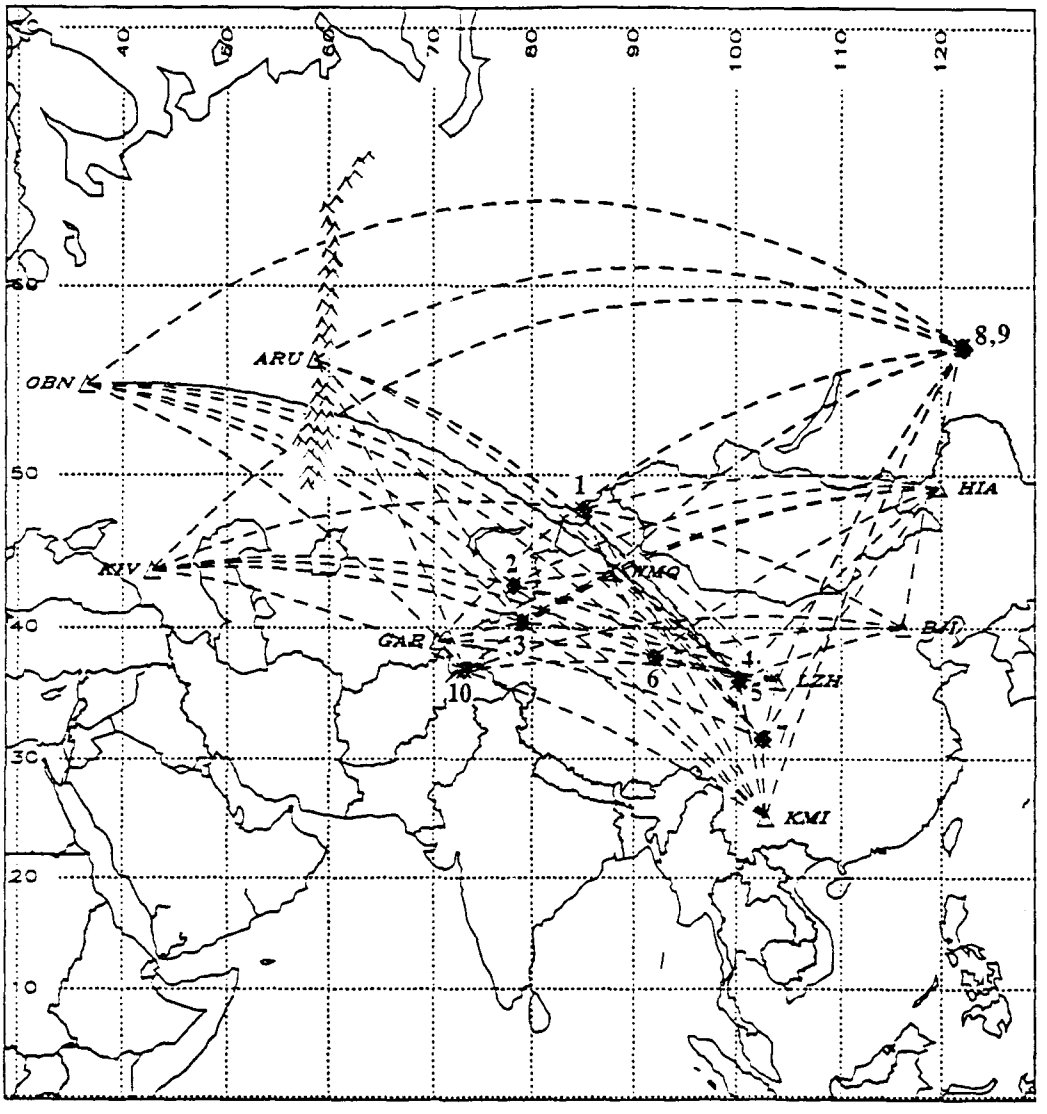

Figure 1. L_g great-circle paths linking the epicentral locations of the ten selected earthquakes (Table 1) and the IRIS/CDSN stations.

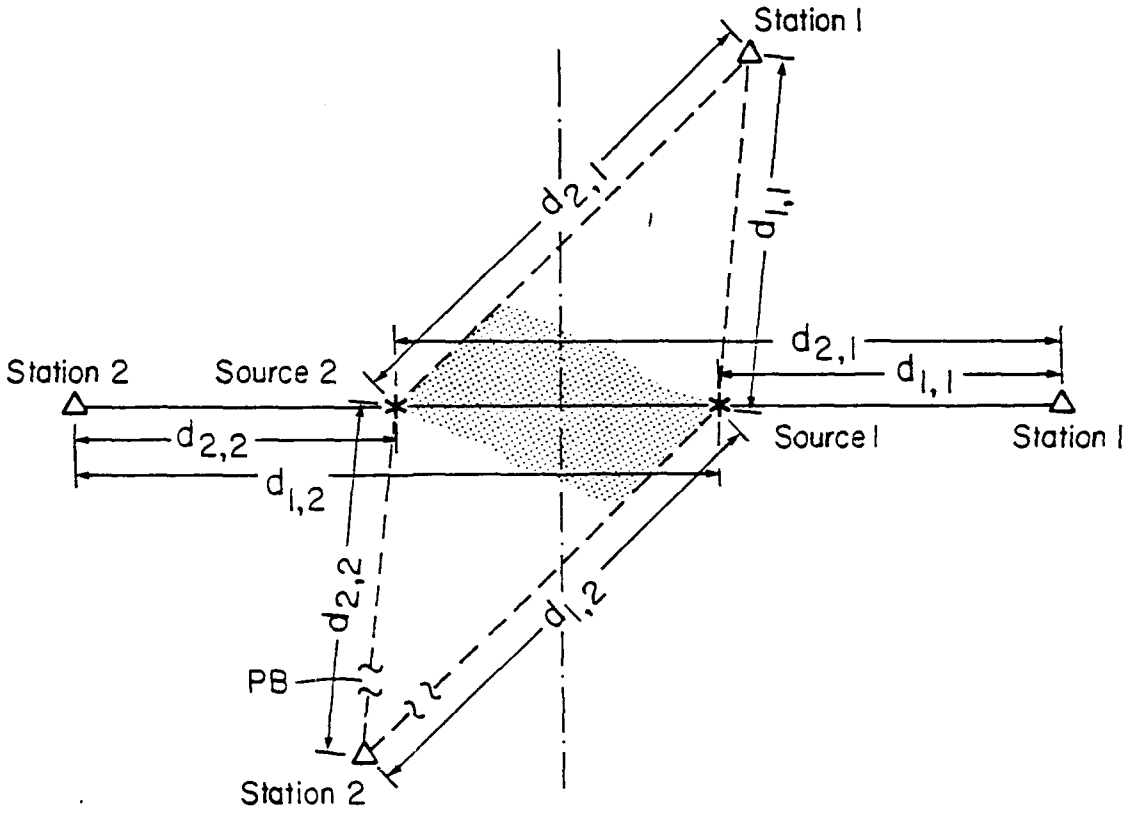

$$\left(\frac{A_{2,1}}{A_{1,1}}\right)\left(\frac{A_{1,2}}{A_{2,2}}\right)=\left(\frac{d_{1,1}}{d_{2,1}}\cdot\frac{d_{2,2}}{d_{1,2}}\right)^{\frac{1}{3}}\left(\frac{\sin\Delta_{1,1}}{\sin\Delta_{2,1}}\cdot\frac{\sin\Delta_{2,2}}{\sin\Delta_{1,2}}\right)^{\frac{1}{2}}e^{-\gamma(D_1+D_2)}$$

PB : Partial Blockage

Figure 2. Schematic drawing illustrating the source pair/receiver pair (SPRP) method for measuring L_g attenuation. Solid horizontal line shows an ideal great-circle alignment; dashed lines show the "generalized" configuration which is actually used in the study. The ideal configuration allows cancellation of the source radiation effects; the generalized configuration does not.

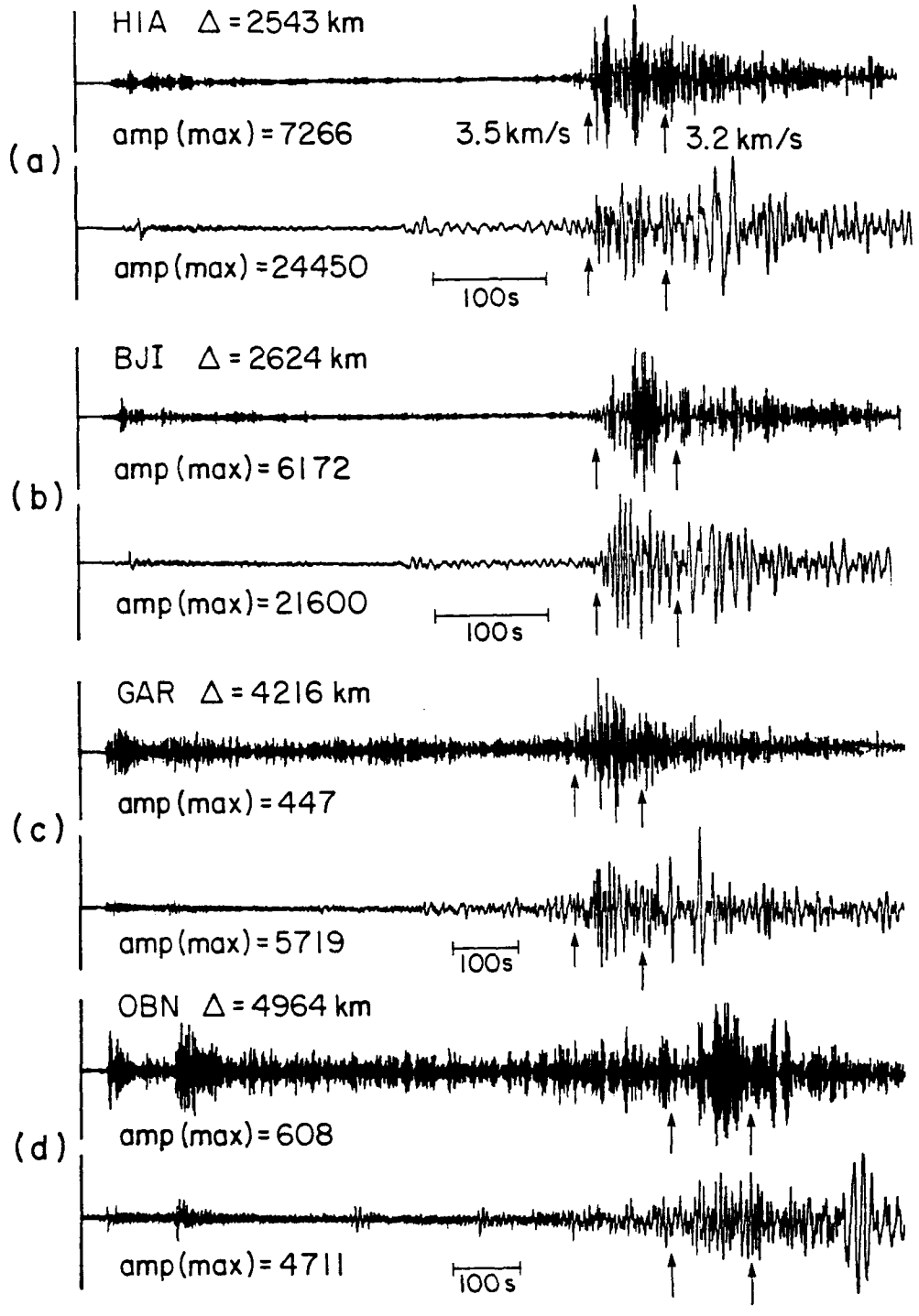

Figure 3. Vertical-component seismograms from CDSN (HIA and BJI) and IRIS (GAR and OBN) stations. For each of the four pairs, the upper trace is the filtered (0.375 - 0.625 Hz band) record and the lower trace the original record.

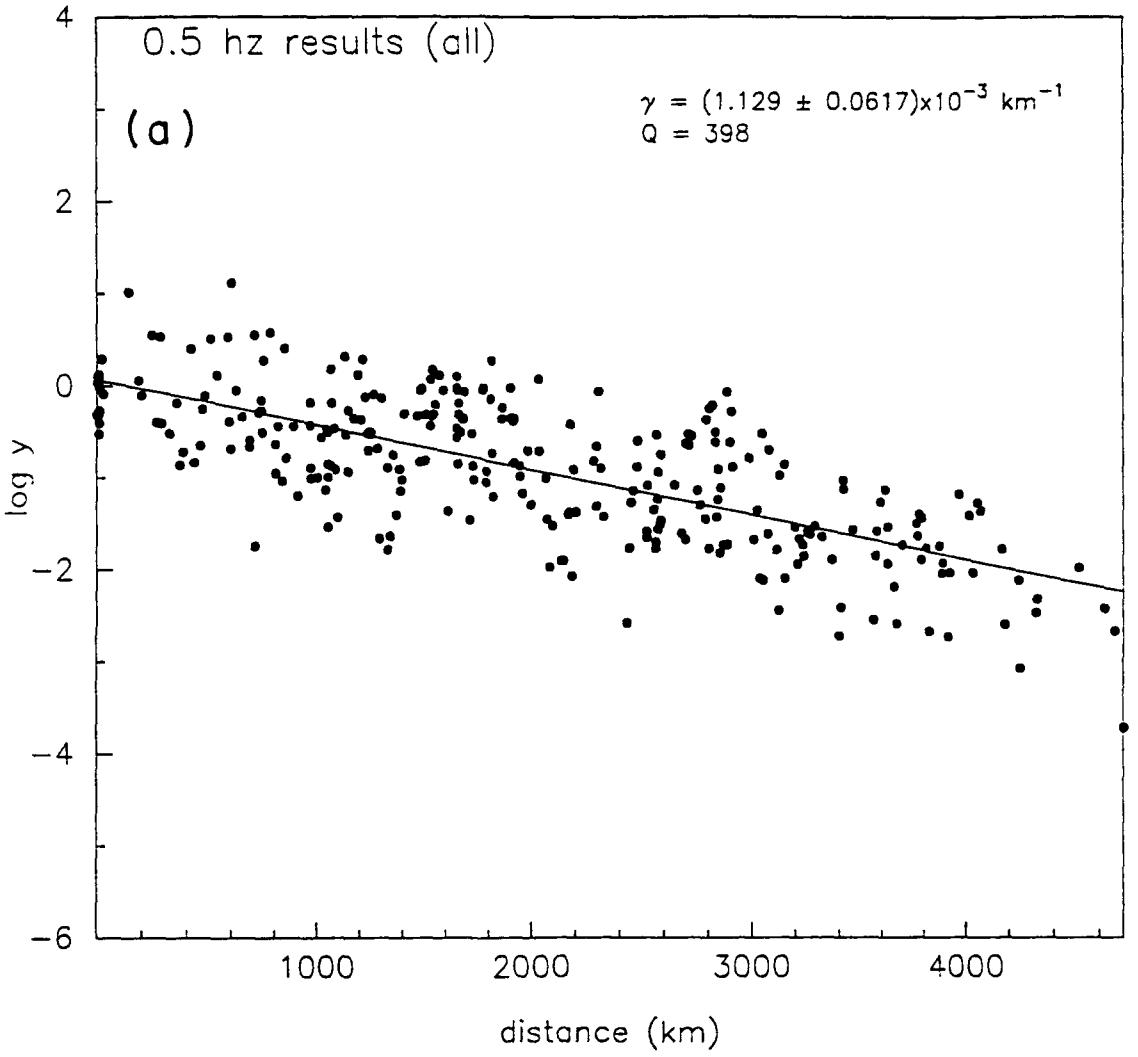

Figure 4. log$Y$ (lefthand side of equation 4) plotted as a function of D (see text). The slope of the least-squares line is -$loge \times \gamma$. The result derived from all 73 paths is shown in 4a; the result derived from 65 selected paths (see text) is shown in 4b. The latter is our preferred result.

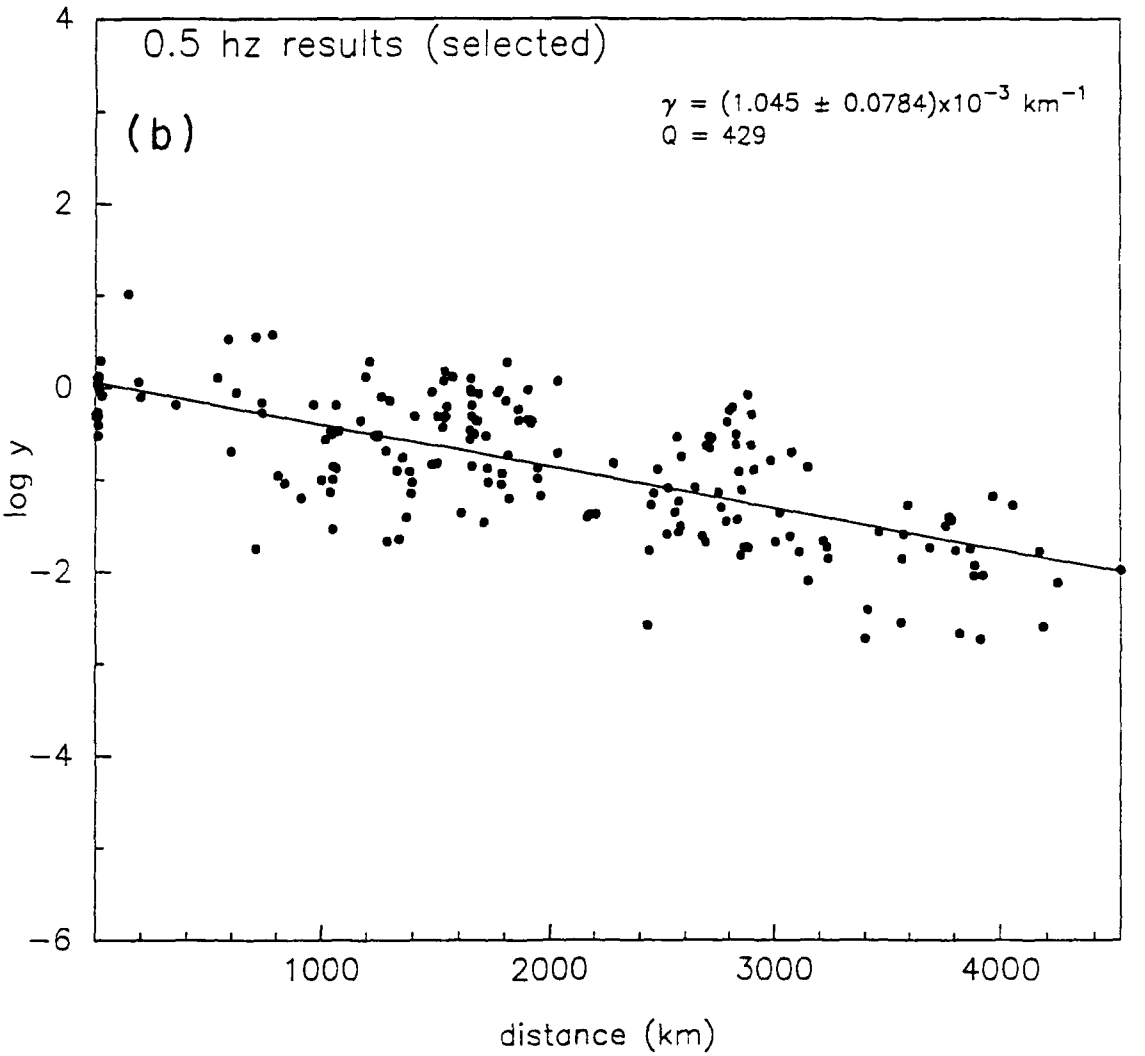
0.5 hz results (selected)
(b)
γ = (1.045 ± 0.0784)x10^-3 km^-1
Q = 429
log y
distance (km)
4
2
0
−2
−4
−6
1000
2000
3000
4000

Figure 4b